Journal of Visualized Experiments

Tetrameric fluorescent antigen arrays for single-step identification of antigen-specific B cells

--Manuscript Draft--

Article Type:	Invited Methods Article - JoVE Produced Video
Manuscript Number:	JoVE61827R2
Full Title:	Tetrameric fluorescent antigen arrays for single-step identification of antigen-specific B cells
Corresponding Author:	J. Daniel Griffin University of Kansas Lawrence, KS UNITED STATES
Corresponding Author's Institution:	University of Kansas
Corresponding Author E-Mail:	jdgriffin@ku.edu
Order of Authors:	Kyle D. Apley
	J. Daniel Griffin
	Stephanie N. Johnson
	Cory J. Berkland
	Brandon J. DeKosky
Additional Information:	
Question	**Response**
Please indicate whether this article will be Standard Access or Open Access.	Standard Access (US$2,400)
Please indicate the **city, state/province, and country** where this article will be **filmed**. Please do not use abbreviations.	Lawrence, Kansas, United States
Please confirm that you have read and agree to the terms and conditions of the author license agreement that applies below:	I agree to the Author License Agreement
Please specify the section of the submitted manuscript.	Immunology and Infection
Please provide any comments to the journal here.	We reuploaded the figures as a preferred format (.svg), but we were unable to denote them as figures in the selection menu.

Dear Jaydev,

We are pleased to share our report, entitled *"Tetrameric fluorescent antigen arrays for single-step identification of antigen-specific B cells"* with you for the upcoming "Methods for Elucidating Action Mechanisms of Immunotherapies" special edition in JoVE.

This methods protocol details the fabrication and use of B cell probes for the identification of antigen specific B cells. While other methods exist toward these ends, we submit this protocol as an innovation of prior art that enables the single step labeling of target B cell populations. By grafting antigen onto a polymeric, water soluble tetrameric backbone, we demonstrated the improvement of physicochemical antigen properties that enables an avid engagement of cognate B cell receptors for highly specific fluorescent labeling.

We prepared this manuscript to share our platform as a customizable tool that is readily approachable and implementable by laboratories spanning a wide variety of disciplines. We look forward to your careful review of this demonstration.

Best,

Danny Griffin
jdgriffin@ku.edu

TITLE:

Tetrameric Fluorescent Antigen Arrays for Single-Step Identification of Antigen-Specific B Cells

AUTHORS AND AFFILIATIONS:

Kyle D. Apley[1,*], J. Daniel Griffin[1,*], Stephanie N. Johnson[1], Cory J. Berkland[1,2,3], Brandon J. DeKosky[1,2,3]

[1]Department of Pharmaceutical Chemistry, University of Kansas, Lawrence, KS, USA
[2]Bioengineering Graduate Program, University of Kansas, Lawrence, KS, USA
[3]Department of Chemical and Petroleum Engineering, University of Kansas, Lawrence, KS

*These authors contributed equally.

Email addresses of co-authors:

Kyle D. Apley	(kdapley@ku.edu)
J. Daniel Griffin	(jdgriffin@ku.edu)
Stephanie N. Johnson	(stephanienjohnson@ku.edu)
Cory J. Berkland	(berkland@ku.edu)

Corresponding author:

Brandon J. DeKosky	(dekosky@ku.edu)

KEYWORDS:

antigen-specific, bioconjugation, fluorescent probes, flow cytometry, assay development, B cells

SUMMARY:

This protocol details the customizable production and use of fluorescent probes for labeling antigen-specific B cells.

ABSTRACT:

Fluorescent antigen production is a critical step in the identification of antigen-specific B cells. Here, we detailed the preparation, purification, and the use of four-arm, fluorescent PEG-antigen conjugates to selectively identify antigen-specific B cells through avid engagement with cognate B cell receptors. Using modular click chemistry and commercially available fluorophore kit chemistries, we demonstrated the versatility of preparing customized fluorescent PEG-conjugates by creating distinct arrays for proteolipid protein ($PLP_{139-151}$) and insulin, which are important autoantigens in murine models of multiple sclerosis and type 1 diabetes, respectively. Assays were developed for each fluorescent conjugate in its respective disease model using flow cytometry. Antigen arrays were compared to monovalent autoantigen to quantify the benefit of multimerization onto PEG backbones. Finally, we illustrated the utility of this platform by isolating and assessing anti-insulin B cell responses after antigen stimulation ex vivo. Labeling insulin-specific B cells enabled the amplified detection of changes to co-stimulation (CD86) that were otherwise dampened in aggregate B cell analysis. Together, this report enables the production and use of fluorescent antigen arrays as a robust tool for probing B cell populations.

INTRODUCTION:

The adaptive immune system plays a critical role in the progression or regression of many disease states, including autoimmunity, cancer, and infectious diseases[1]. For broad applications including the study of immunopathology or the development of new precision treatments, it is often critical to assess antigen-specific B and T cell responses underlying disease progression[2-4]. Major histocompatibility complex (MHC) tetramers are widely and commercially available for identifying antigen-specific T cell clones[5]. These fluorophore-labeled constructs present quadrivalent peptide-MHC complexes to avidly engage with cognate T cell receptors for labeling applications such as microscopy and flow cytometry.

Antigens for B cell interrogation can present highly varied molecular weights, charges, and solubilities[6,7]. When using monomeric antigen as soluble B cell probes, physicochemical antigen properties may not be stabilized through complexing with the much larger, water soluble streptavidin molecule, or could present solubility issues as monomeric reagents prior to conjugation. Thus, some proteins present bioconjugation difficulties and unexpected results in practice[7,8]. Direct fluorescent dye conjugation can sometimes render constructs water insoluble and lipophilic. These direct dye-antigen compounds are susceptible to nonspecific embedding within cell membranes, confounding antigen-specific analyses[7-9]. Some strategies have overcome solubility challenges by coupling antigen and fluorophores with other functional groups. Cambier et al., for example, employed biotinylated insulin in its native form to engage with insulin-specific B cell receptors (BCRs) before adding fluorophore-labeled streptavidin in a stepwise fashion[10]. While this approach enabled the assessment of B cells that bind to monomeric insulin with high resolution, two labeling steps were required. A generalizable protocol for the preparation of ready-to-use polymer-based B cell probes that is readily integrated with common fluorescent antibody labeling procedures would be of benefit for furthering the study of B cells in disease.

In this protocol, we detail the production and use of fluorescent antigen arrays (FAAs) for the generalizable and single-step labeling of antigen-specific B cells for microscopy and flow cytometry experiments (**Figure 1**). Soluble antigen arrays (SAgAs) have been employed over the past decade as B cell-targeted antigen-specific immunotherapies against autoimmune diseases[11-22]. SAgAs leverage multivalent antigen display on flexible, polymeric backbones to avidly engage B cell receptors and elicit immunomodulatory effects, though their antigen-specificity provides another opportunity for probing B cells of interest when coupled to a fluorophore[23]. The polymeric backbones constituting SAgAs confer water solubility to the overall biomacromolecule and can dampen the sometimes extreme antigen characteristics that confound probe generation and staining specificity[6,24]. We have grafted numerous antigens ranging in size and complexity onto SAgA platform using modular click chemistry, which is conducive to the use of small peptide epitopes and full proteins[14,18]. Here, we demonstrate FAAs as robust antigen-specific B cell labeling tools that can be used in parallel with typical fluorescent antibody labeling. We prepared and evaluated FAAs consisting of human insulin for labeling B cells in a transgenic mouse model of Type 1 Diabetes (VH125), as well as FAAs that incorporated proteolipid protein 139-151 (PLP), a peptide epitope for experimental autoimmune encephalomyelitis (EAE), the mouse model of Multiple Sclerosis. Our intention in employing these disease models was to demonstrate the

versatility of this platform, both for the modular substitution of antigens used, as well as the viability of use with peptide epitopes (PLP) and full proteins (insulin) alike. This protocol is presented with the purpose of accessibility, without extensive bioconjugation expertise required. The reagents, as well as synthesis and purification methods, are designed to be versatile and readily implemented at most research labs focused in chemistry, molecular biology, or immunology.

PROTOCOL:

All animal procedures represented in this work were approved by the Institutional Animal Care and Use Committee at the University of Kansas.

1. Antigen array synthesis (4–6 days)

1.1. Functionalize unmodified antigen with an alkyne handle (1 h). Add 1 equivalent insulin (100 mg, 17.4 µmol) to a 20 mL glass vial with a stir bar and dissolve in anhydrous dimethylsulfoxide (DMSO) (2 mL) with gentle heating to 40–50 ˚C using a heat-gun or water bath.

1.1.1. Add 1,1,3,3-tetramethylguanidine (40.2 mg, 348.8 µmol) and 1.35 equivalents freshly prepared 78.5 mM propargyl N-hydroxysuccinimide ester (NHS-ester) stock solution in anhydrous DMSO (0.3 mL, 5.3 mg, 23.6 µmol).

1.1.2. Stir for 30 min at room temperature then quench the reaction with 0.05% HCl (12 mL).

1.2. Purify the singly modified insulin-alkyne by reverse-phase liquid chromatography (4 h). Use a preparative C18 column (19 mm x 250 mm, 300 A pore size, 5 µm particle size) with a 10 min 30–40% B gradient (A, water with 0.05% trifluoroacetic acid (TFA); B, acetonitrile with 0.05% TFA) and a flow rate of 14 mL/min. The desired product elutes immediately after unmodified insulin.

1.2.1. Evaporate acetonitrile and TFA by nitrogen gas stream or rotary evaporation under reduced pressure (650 Pascals) and rotating at 150 rpm. Freeze the aqueous solution and lyophilize to dryness. Store functionalized insulin at -20 ˚C under a dry atmosphere.

NOTE: The functionalized insulin is stable for up to a year under these storage conditions.

1.3. Synthesize the antigen array by copper-catalyzed, azide-alkyne cycloaddition (CuAAC) (2.5 h)[22]. Add 6 equivalents insulin-alkyne (38 mg, 6.3 µmol) to a 10 mL glass vial with a stir bar and dissolve in DMSO (1.2 mL) with gentle heating.

1.3.1 Add 50 mM sodium phosphate buffer (1.8 mL) pH 7.4, 1 equivalent 20 kDa 4-arm PEG azide (21 mg, 1.05 µmol), copper (II) sulfate pentahydrate (3.15 mg, 12.6 µmol), Tris(3-hydroxypropyltriazolylmethyl)amine (27.37 mg, 63 µmol), and sodium ascorbate (50.34 mg, 254 µmol).

1.3.2. Stir for 2 h at room temperature then add DMSO (3 mL) to solubilize any precipitates and acidify the solution with 0.05% HCl (4 mL).

1.4. Purify the antigen array by reverse-phase liquid chromatography (3 h). Use a preparative C18 column (19 mm x 250 mm, 300 A pore size, 5 µm particle size) with a 10 min 20–60% B gradient (A, water with 0.05% TFA; B, acetonitrile with 0.05% TFA) and a flow rate of 14 ml/min. The desired product elutes immediately after insulin-alkyne.

1.4.1. Evaporate acetonitrile by nitrogen gas stream or rotary evaporation under reduced pressure. Freeze the aqueous solution and lyophilize to dryness. Store at -20 ˚C under a dry atmosphere.

NOTE: The insulin antigen array is highly hygroscopic. The lyophilized fibers may coalesce into a dense pellet after repeated exposure to the atmosphere. FAA properties may differ depending on the application-specific antigen used. The insulin antigen array is stable for several months under these storage conditions.

2. Fluorophore conjugation (1–2 days)

2.1. Conjugate the fluorophore to the antigen array (2.5 h). Add 1 equivalent tetravalent insulin (21.7 mg, 0.5 µmol) to a 20 mL glass vial with stir bar and dissolve in DMSO (1.75 mL) with gentle heating. Add freshly prepared 100 mM carbonate buffer (8 mL) pH 9.0 and 5 equivalents of fluorescein isothiocyanate in a freshly prepared 10 mM stock solution in DMSO (0.25 ml, 0.97 mg, 2.5 µmol). Stir for 2 h in the dark at room temperature.

2.2. Purify the product by dialysis (24 h). Use 3.5 kDa molecular weight cutoff dialysis tubing in a stirred 5 L bucket with distilled water in the dark at room temperature. Dialyze for 24 h and change the dialysis solution every 6–12 h.

2.3. Freeze the dialyzed solution and lyophilize to dryness to yield the FAA. Store in the dark under a dry atmosphere at -20 ˚C.

NOTE: The FAA is stable for several months under these storage conditions.

3. FAA characterization (2–4 h)

3.1. Analyze the products of steps 1 and 2 by sodium dodecyl sulfate-polyacrylamide gel electrophoresis according to Laemmli[25] (2 h). Prepare samples containing 5 µg of purified monovalent antigen, 20 kDa 4-arm PEG azide, antigen array, and FAA.

3.1.1. Visualize fluorophore labeling in the FAA samples by fluorescence imaging in a gel-imager.

3.1.2. Perform Coomassie blue staining[26] to visualize the antigen.

3.1.3. Perform iodine staining[27] to visualize the PEG backbone. Rinse the gel in distilled water (3 x 2 min), incubate in 5% barium chloride solution (20 mL) for 10 min, rinse in distilled water (3 x 2 min), incubate in 0.1 N iodine solution (20 mL) for 1 min, then rinse in distilled water (3 x 2 min) to remove background staining before visualization.

NOTE: To make 0.1 N iodine solution, add potassium iodide (2.0 g, 12 mmol) and iodine (1.27 g, 5 mmol) to 100 mL distilled water.

3.2. Calculate the degree of dye-labeling by UV-Vis spectroscopy (1 h). Dissolve a small amount of FAA at 0.1 mg/mL and record the absorbance at 280 nm and the peak absorption wavelength for the dye. Obtain the molar extinction coefficients for the antigen and the dye.

NOTE: Some dyes are pH sensitive. Make sure to use an appropriately buffered solution like100 mM carbonate buffer with pH 8.3 when measuring the FAA absorbance to ensure the reported dye extinction coefficient is accurate.

3.2.1. Perform the following calculation[28] where $A_{Dye,\ max\lambda}$ is the FAA absorbance at the peak absorption wavelength for the dye, $E_{Dye,\ max\lambda}$ is the molar extinction coefficient at the peak absorption wavelength for the dye, and $E_{antigen,\ 280\ nm}$ is the molar extinction coefficient for monovalent antigen at 280 nm.:

Correction Factor (CF) = $A_{Dye,\ 280\ nm}$ / $A_{Dye,\ max\lambda}$

$0.25 * (A_{Dye,\ max\lambda} / E_{Dye,\ max\lambda}) * (E_{antigen,\ 280\ nm} / (A_{280\ nm} – (A_{Dye,\ max\lambda} * CF))) = dye/FAA$

3.3. Analyze the FAA for free dye or potential degradation products by RP-HPLC (1 h).

3.3.1. Dissolve a small amount of FAA at 1.0 mg/mL and analyze with an analytical C18 column (4.6 mm x 150 mm, 300 A pore size, 2.5 µm particle size) using a 10 min 5–95% B gradient (A, water with 0.05% trifluoroacetic acid: B, acetonitrile with 0.05% trifluoroacetic acid) with a flow rate of 1 mL/min. Set the UV-Vis detector to monitor the peak absorbance wavelength of the dye (437 nm for FITC).

NOTE: For pH sensitive dyes, HPLC analysis in acidified solvents may require shifting the monitored wavelength from the dye's peak absorption wavelength in neutral, aqueous conditions. In 0.05% TFA, the pH is approximately 3 and the max absorption for FITC has shifted.

4. Assay development by FAA titration (3–5 h)

NOTE: FAA use for flow cytometry is presented, but the same steps can be modified for use in other formats such as immunohistochemistry or fluorescent microscopy. When applying FAAs for a new format, a new optimization assay must be completed. Mixed or isolated cell populations may be obtained through blood or lymphoid organ processing methods[23,29]. Harvest through enzymatic digestion of tissue is not recommended, as cells surface markers may be shed.

4.1. Suspend FAA stock to 1 mg/mL in FACS buffer (1x PBS + 5% fetal bovine serum and 0.1% sodium azide). Up to 10% DMSO can be incorporated to accelerate dissolution.

4.2. Obtain cells positive for antigen-specific B cells of interest and dispense into microcentrifuge tubes. Approximately 1 x 10^7 total cells will be required.

NOTE: Splenocytes were harvested from VH125 and EAE mice according to IACUC-approved protocols at the University of Kansas for the present demonstration. Researchers may employ the methods described herein for cell samples specific to their own application and FAA preparation.

4.2.1. Dispense 5 x 10^5 cells for titration labeling replicates (at least 3 replicates per titration).

4.2.2. Dispense 1 x 10^5 cells for single-stain controls as well as an unstained control.

NOTE: Antibody isotypes and fluorescence minus one control may also be used to fully validate the assay.

4.3. Wash cells by adding 1 mL of FACS buffer to each tube. Centrifuge at 200 x *g* for 5 min.

4.4. Aspirate the supernatant and resuspend cell pellets in 50 µL of FACS buffer.

4.5. Add CD3 and CD19 fluorescent antibodies to each sample at manufacturer recommended concentrations, as well as titrated FAA doses.

NOTE: Fluorescent antibody working concentrations may be titrated independently to confirm the lot integrity. Appropriate FAA dose ranges will vary by application, but a good starting point is 50, 25, 10, 5, and 1 µg per sample. 1 µL of stock FAA solution equals 1 µg of dose.

4.6. Mix each sample well and incubate covered from light, on ice for 30 min.

4.7. After the incubation, wash cells by adding 1 mL of FACS buffer to each tube. Centrifuge the samples at 200 x *g* for 5 min.

4.8. Aspirate the supernatant and repeat the wash by adding 1 mL of FACS buffer to each tube. Centrifuge the samples at 200 x *g* for 5 min.

4.9. Aspirate the supernatant and resuspend the samples in 200 µL of fresh FACS buffer. Place the samples on ice and head to the cytometer.

4.10. Run the samples on the cytometer and collect at least 50,000 events.

5. FAA titration analysis and labeling dose optimization (1–2 h)

5.1. Using flow cytometry analysis software, gate for single cells.

5.2. On single cells, place gates for CD19+ (B cells) and CD3+ (T cells).

5.3. Within CD19+ and CD3+ parent populations, gate for FAA+ events in the relevant fluorochrome channel.

5.4. Record the percentage of FAA+ events within the CD19+ and CD3+ parent populations.

5.5. Calculate a specificity ratio by dividing the proportion of FAA+ events in the CD19+ population (specific) by the proportion of FAA+ events in the CD3+ population (nonspecific). Specificity ratio should be maximized for successful FAA use.

5.6. Employ the labeling dose corresponding to the highest specificity ratio for future experiments.

REPRESENTATIVE RESULTS:

The purified yield of insulin-alkyne (**Figure 2**, upper panel), determined by weight, typically varied from 50–65%. Yields of less than 40% were likely caused by water contamination in the anhydrous DMSO and or hydrolysis of the propargyl NHS-ester. For antigen multimerization (**Figure 1B**), the purified yield of the insulin antigen array (**Figure 2**, middle panel) varied from 60–75% and SDS-PAGE analysis confirmed the major product was the tetravalent species (**Figure 3A**). For fluorophore modification (**Figure 1C**), the purified yield of FITC 4-arm insulin FAA (**Figure 2**, lower panel) was consistently near 50%. Analysis by SDS-PAGE qualitatively confirmed dye conjugation to the tetravalent antigen array (**Figure 3A**). Analysis of FITC 4-arm insulin by HPLC at the peak absorption wavelength for FITC in acidic conditions, 437 nm, confirmed the removal of free dye (**Figure 3B**) from the material. Analysis of FITC 4-arm insulin by HPLC at 280 nm (**Supplementary Figure 1A**) showed a downfield peak shift that corresponds to the retention time of the FITC 4-arm insulin peak at 437 nm. Although the change in retention time is slight, the homogeneity of the 280 nm FITC 4-arm insulin peak supports near unity dye-labeling of the insulin antigen array. The degree of dye labeling for FITC 4-arm insulin was calculated to be 1.52 (**Supplementary Table 1**) from the absorbance spectrum (**Figure 3C**).

Rhodamine B (RhdB) insulin, FITC PLP, and RhdB 4-arm PLP FAAs were also synthesized. The purified yield of PLP antigen array was 47% after 20 h using 4.25 equivalents PLP-alkyne. The multimerization reaction was monitored by HPLC and demonstrated that using fewer equivalents of antigen-alkyne required longer reaction times. The fluorophore conjugation reactions were performed for all FAAs in identical conditions. The degree of dye-labeling was calculated for each FAA (**Supplementary Table 1**) from their respective absorbance spectrums (**Supplementary Figure 3**) and purity was evaluated by HPLC (**Supplementary Figure 1** and **Supplementary Figure 2)** The degree of dye-labeling for RhdB insulin, FITC PLP, and RhdB 4-arm PLP was 0.25, 2.54, and 0.1, respectively. The low degree of dye-labeling for RhdB insulin and RhdB PLP, as calculated from the absorbance spectrum, was unexpected and conflicts with the near-complete conversion of insulin and PLP antigen arrays to a new species observed by HPLC (**Supplementary Figure 1B**

and **Supplementary Figure 2B**). The HPLC spectra for each FAA (**Supplementary Figure 1** and **Supplementary Figure 2**) demonstrated the purity of the final product. All FAAs besides the RhdB 4-arm insulin were entirely free of non-conjugated dye. The purified RhdB 4-arm insulin had free dye present that contributed to 20% of the area under the curve in the 555 nm spectra. While this amount of free dye did not hamper its utility in flow cytometry assays, dialysis should be continued to fully remove the free dye in order to calculate the degree of labeling by UV-vis spectroscopy.

In the examples provided, FAA variants were constructed using human insulin and PLP. Human insulin is the cognate antigen for VH125 NOD mouse splenocytes, a transgenic line harboring 1-3% insulin-specific B cells (IBCs) within the total B cell pool[30]. PLP is an encephalitogenic peptide epitope used to induce EAE, a murine model of multiple sclerosis. Antibodies are generated against the PLP epitope in this model, indicating a B cell response[31]. These models were each employed to demonstrate FAA utility for full protein antigens and antigenic epitopes alike.

Assay development by FAA titration was carried out for FITC 4-arm insulin and RhdB 4-arm PLP in their cognate cell populations (**Figure 4**, **Supplementary Figures 4–7**). VH125 mice were bred at the University of Kansas under institutional animal care and use (IACUC) guidelines and splenocytes were harvested from a male at approximately 30 weeks of age. EAE cells were obtained from 4–6-week-old female SJL/J mice 14 days after inducing the disease under IACUC-approved guidelines. Staining differences were appreciable between CD19+FAA+ IBCs and CD3+FAA+ T cells in VH125 splenocytes (**Figure 4**). A distinct FAA population was evident among CD19+ cells, while nonspecific FAA+ staining among CD3+ T cells was more of a smear that was minimized at low labeling dose (**Figure 4A,B**). By compiling specificity ratios at each tested dose, we showed that the specificity was highest at a labeling concentration of 0.02 mg/mL (**Figure 4C**). Similar success was harnessed for probing PLP-specific B cells in the EAE model, where a 0.1 mg/mL labeling dose was optimized (**Supplementary Figure 6** and **Supplementary Figure 7D**). However, PLP-specific staining in EAE splenocytes was not as distinct as was observed with insulin-specific staining in the VH125 cells.

The benefit of antigen multimerization on a polymeric backbone was assessed by comparing IBC staining using FITC 4-arm insulin compared to monovalent RhdB insulin in the same flow cytometry panel at 0.02 mg/mL each (**Figure 4D, Supplementary Figure 8**). Parallel analysis uncovered that 4-arm antigen provided higher staining of the IBC population that was better separated from the FAA negative cells for improved specificity (**Supplementary Figure 8**). These data showed that roughly half of IBCs would have been unidentified if RhdB insulin was used alone, despite a higher molar amount of the monovalent antigen at 0.02 mg/mL.

After titrating insulin and PLP FAAs for flow cytometry, we conducted a mock antigen stimulation assay to assess robustness for practical application using FITC-labeled FAAs (**Figure 5**, **Supplementary Figures 9–11**). After challenging VH125 or EAE splenocytes for 24 hours with or without 10 μg/mL of cognate antigen (insulin or PLP, respectively), FAA+ populations were gated on $FITC_{hi}$+ scatter (**Supplementary Figures 9–10**). Differences in antigen-specific B cell prevalence could be assessed directly (**Figure 5A, Supplementary Figure 11A.**), but the most notable use for

FAAs was evident in analyzing cell phenotype changes within antigen-specific B cell populations (**Figure 5B,C,** and **Supplementary Figure 11B,C**), revealing statistically significant cellular changes that are obscured during analysis of splenocyte population data. In this application demonstration, CD86 (costimulation) was assessed as a model biomarker that responds to antigen stimulation (commercially available fluorescent antibodies were employed for the analysis)[22,32]. CD86 is upregulated when B cell receptors engage with cognate autoantigen, so we hypothesized that changes in this marker would be enhanced in antigen-specific B cells after antigen challenge. Mean fluorescence intensity (MFI) was slightly elevated upon antigen challenge in VH125 and EAE splenocytes, but these increases were concentrated in antigen-specific B cells (**Figure 5B, Supplementary Figure 11B**). Further, antigen-specific B cells were consistently observed to present higher levels of the CD86 costimulatory marker than the rest of the B cell pool. These data validated FAAs as powerful tools for probing disease-relevant changes in adaptive immune-mediated disorders.

FIGURE AND TABLE LEGENDS:

Figure 1: Overview of custom FAA generation as fluorescent B cell probes. (**A**) The desired protein or peptide epitopes are selected for antigen-specific B cell detection. (**B**) Copper (I) catalyzed azide-alkyne cycloaddition facilitates the quadrivalent multimerization of antigen onto 4-arm PEG polymer backbones. (**C**) 4-arm PEG with conjugated antigens are modified with fluorophore at an average of one equivalent per polymer backbone. (**D**) Purified fluorescent antigen arrays are titrated and validated in biological assays to analytically interrogate antigen-specific B cells.

Figure 2: Reaction synthesis pathways for generating FAAs. These reaction conditions support a broad range of protein and fluorophore conjugates. The synthesis of FITC-insulin FAAs is shown as an example.

Figure 3: Synthesis and purification results for insulin FAAs. The insulin antigen array and FITC insulin FAA were analyzed for purity and characterized to determine the degree of dye-labeling. (**A**) The samples analyzed by SDS-PAGE are: 1, ladder; 2, insulin-alkyne; 3, 20 kDa 4-arm PEG azide; 4, 1.3. t = 1 min; 5, 1.3. t = 10 min; 6, 1.3. t = 60 min; 7, 1.3. t = 120 min; 8, purified insulin antigen array; 9, FITC 4-arm insulin FAA. Gels were stained with (left) Coomassie Blue to visualize protein, (middle) Coomassie Blue and iodine to visualize protein and PEG, and (right) fluorescence imaging to visualize dye. (**B**) FITC 4-arm insulin FAA was analyzed by HPLC at 437 nm to determine purity. (**C**) FITC 4-arm insulin FAA (0.01 mg/mL) and insulin antigen array (0.01 mg/mL) were analyzed by UV-Vis spectroscopy to calculate the degree of dye-labeling.

Figure 4: Representative results for titrating FAAs for flow cytometry assay development. (**A**) Specific positive events were gated among B cells (CD19+) for a range of labeling titrations. (**B**) The same analysis was performed by gating in a T cells (CD3+) that nonspecifically bound FAAs. (**C**) FAA+ of CD19+ (specific) events were divided by FAA+ of CD3+ (nonspecific) events at each titration to yield a specificity ratio, which was optimized for further application-specific FAA use. (**D**) Antigen-specific B cell labeling was compared between FAAs and monovalent fluorescent antigen. Results were compared using a two-tailed, unpaired t test (n = 3/group, *p < 0.05, **p

< 0.01).

Figure 5: Demonstration of FAA screening in an animal model of Type I diabetes. Transgenic VH125 splenocytes were incubated with 10 μg/mL of insulin or media alone (vehicle) for 24 h. (**A**) FAAs were used to quantify insulin-specific B cells among the CD19+ population between the treatments. (**B**) Gating on insulin-specific B cells (right) enabled the quantification of CD86 MFI in comparison to aggregate CD19+ data (left). All statistical analyses were conducted using two-tailed, unpaired t tests (n = 6/group, *p < 0.05, **p < 0.01, ***p < 0.001, ****p < 0.0001).

Supplementary Figure 1: HPLC analysis of 4-arm insulin FAAs to evaluate dye conjugation and purity. (**A**) HPLC chromatograms of FITC 4-arm insulin FAA at 437 nm (upper) and at 280 nm (lower). (**B**) HPLC chromatograms of RhdB 4-arm insulin FAA at 555 nm (upper) and at 280 nm (lower).

Supplementary Figure 2: HPLC analysis of 4-arm PLP FAAs to evaluate dye conjugation and purity. (**A**) HPLC chromatograms of FITC 4-arm PLP FAA at 437 nm (upper) and at 280 nm (lower). (**B**) HPLC chromatograms of RhdB 4-arm PLP FAA at 555 nm (upper) and at 280 nm (lower).

Supplementary Figure 3: Analysis of FAAs by UV-Vis spectroscopy to calculate the degree of dye labeling for each FAA.

Supplementary Table 1: Constants values used to calculate the degree of dye labeling for each FAA.

Supplementary Figure 4: Representative gating for the flow cytometry studies. Examples of splenocyte gating (left), singlet isolation (center), and CD19/CD3 gating (right) are provided.

Supplementary Figure 5: Representative titration data for FITC 4-arm insulin in VH125 splenocytes are presented across the full range of concentrations from 0.5 (left) to 0.02 (right) mg/mL in CD19+ (upper) and CD3+ (lower) cells.

Supplementary Figure 6: Representative titration results for rhodamine 4-arm PLP in EAE splenocytes are presented across the full range of concentrations from 0.5 (left) to 0.02 (right) g in CD19+ (upper) and CD3+ (lower) cells.

Supplementary Figure 7: Representative specificity ratio analysis among FAAs for VH125 and EAE splenocytes. (**A**) FITC 4-arm insulin labeled cells as a percentage of parent CD19+ (left) or CD3 (right) VH125 cells. (**B**) Specificity ratio (FAA+ of CD19+/FAA+ of CD3+) was calculated for each labeling dose. (**C**) Rhodamine 4-arm PLP labeled cells as a percentage of parent CD19+ (left) or CD3 (right) EAE cells. (**D**) Specificity ratio (FAA+ of CD19+/FAA+ of CD3+) was calculated for each labeling dose. (n = 3/group)

Supplementary Figure 8: Monovalent antigen labeling was directly compared with FAA for specific (left) and nonspecific (right) binding (n = 3). Quadrant 3 is encompassed on the left plot

by a blue box to highlight the population of IBCs that is identified by FAAs, but not monovalent insulin.

Supplementary Figure 9: Representative flow cytometry gating used for splenocyte assays. (**A**) FAA+ (FITC+) cells were identified among vehicle-treated (left) and insulin-treated (right) B cells (VH125). (**B**) FAA+ (FITC+) cells were identified among vehicle-treated (left) and PLP-treated (right) B cells (EAE) (n = 6/group).

Supplementary Figure 10: Single-stain fluorescent labeling. Single-stain fluorescent labeling control samples for the FAA flow cytometry assay shown in Fig. 5 and Supp. Fig. 11. From left to right 5,000 events were collected for unstained splenocytes, and single stain A647-CD19, FITC-FAA, PE/Cy7-CD3, and PE-CD86 splenocytes. Scatter plots are provided signal comparison in the PE/Cy7 and PE channels (upper), and A647 vs. FITC is provided with overlaid FITC+ and FITC- plots to verify minimal spectral overlap between the critical CD19 and FAA markers in our assay (lower).

Supplementary Figure 11: Demonstration of FAA practical utility. EAE splenocytes were challenged with 10 µg/mL of PLP or media alone (vehicle) for 24 h. (**A**) FAAs were used to quantify PLP-specific B cells among the CD19+ population between the treatments. (**B**) Gating on PLP-specific B cells (right) enabled the quantification of CD86 MFI in PLP-specific B cells compared to aggregate CD19+ B cell data (left). All statistical analyses were conducted using two-tailed, unpaired t tests (n = 6/group, *$p < 0.05$, **$p < 0.01$)

DISCUSSION:

We developed a protocol (**Figure 1**) to construct customized FAAs for identifying antigen-specific B cells, simplifying the generation of B cell probes for difficult antigen targets. We selected 4-arm PEG polymers with terminal azide groups as a facile substrate for building FAAs, as PEG confers water solubility while the functional azide handles enable simple click conjugation reactions[33]. The defined number of functional handles (4 arms) is conducive to simplified chemical antigen conjugation because antigen can be used in molar excess to circumvent the need for rigorous reaction optimizations. Researchers building FAAs of their own should consider the need for alkyne functionality when designing antigens. Oligopeptide epitopes can be custom ordered or synthesized with homopropargyl handles from synthetic peptide suppliers. NHS chemistry can also be employed to modify larger protein antigens with alkyne functional groups[18]. If the NHS-esterification in Step 1.1. does not proceed, a likely culprit may be hydrolysis of the NHS-ester. This event can occur if the NHS-ester is not properly stored under a dry atmosphere, or during the reaction if the anhydrous DMSO is contaminated with water. If the copper-catalyzed, azide-alkyne cycloaddition in Step 1.3. fails to produce a tetravalent antigen array, potential solutions include increasing the concentration of reactant antigen or heating to 37 ˚C. If the reaction fails to proceed at all, check that the antigen is free from metal-chelating excipients and oxidizing agents.

We selected a two-step synthesis reaction for FAAs, consisting first of complete antigen occupancy on the PEG backbone followed by modification of one antigen with a fluorophore of

choice. This format simplifies antigen conjugation chemistry, and is conducive to generalized protein labeling chemistries used in commercially-available kits[34]. Antigen modification of some molecules using random chemical conjugation could occlude some antigenic sites, however even bivalent or trivalent ligand presentation markedly increases binding avidity[35, 36]. Ideally, there will be 1 fluorophore per FAA. Varying dye equivalents, antigen array concentrations, and reaction times can be useful to optimize the procedure for specific antigens. If the fluorophore conjugation in Step 2 performs poorly, confirm the carbonate buffer and fluorophore stock solutions were prepared immediately before use, as the pH of carbonate buffers can drift substantially and isothiocyanate or NHS-ester fluorophores will hydrolyze in DMSO if trace water is present. If researchers seek to maximize functional antigen valency, further antigen design variance may be considered, including the addition of charged amino acid residues like lysine in the custom synthesis of peptide epitopes, or through recombinant engineering of protein antigens. A wide variety of fluorophores and dye labeling kits may be selected by researchers based on compatibility with other fluorochromes in assay panels.

A final consideration for synthesis and characterization of FAAs is the use of organic solvents. In the protocol above, DMSO may be omitted from Step 1.3 (antigen multimerization via CuAAC) and Step 2.1 (fluorophore conjugation) without issue, as the solvent is only used to aid in antigen or dye dissolution when poor solubility is observed. For Step 1.1. (antigen functionalization with alkyne handle) switching to a buffered aqueous solution will require increased equivalents of propargyl NHS-ester, as hydrolysis of the NHS-ester will compete with conjugation. Additionally, a more heterogenous product will result as the described reaction conditions promote acylation of the single lysine on insulin over the two n-termini[37]. For larger protein antigens that are unstable in organic solvents, amine-selective acylation reactions performed at neutral pH will favor modification of the n-terminal amine, as n-terminal amines possess lower pKas than lysine side-chains[38]. Further, alkyne functionalized protein antigens may be purified by ion-exchange chromatography to avoid exposure to organic solvents. Purification of antigen arrays containing sensitive antigens can be conducted similarly, or dialysis may be used when oligopeptide epitopes under 2,000 Da are used.

In this report we fabricated 4-arm PEG constructs with either PLP or insulin to demonstrate versatility using peptide and protein antigens (**Figure 3, Supplementary Figures 1–3**). We grafted each variant to either FITC or RhdB dyes to also illustrate fluorochrome customizability (**Figure 3, Supplementary Figures 1–2**). After titrating FAA variants for exposure to cell populations (FITC 4-arm insulin into VH125 splenocytes, RhdB 4-arm PLP into EAE splenocytes), the benefits of FAAs over monovalent antigen were readily apparent. While VH125 B cells labeled with a clear FAA+ population (**Figure 4**), FAA+ B cells from the EAE model were less distinct. This difference may have been due to the lower affinity and/or lower prevalence of PLP-specific B cells in splenocytes from the EAE disease model, which were harvested only 14 days from disease induction[39]. This difference also highlights the fact that the fraction of labeled B cells will differ based on disease model and target BCR affinities. Nonetheless, gating on the “high” staining population in EAE splenocytes led to similar phenotypic B cell changes as with the VH125 analysis when FITC FAAs were used for both models (**Figure 5**, **Supplementary Figure 11**). The clear benefit to FAAs over fluorophore-labeled monovalent antigen was observed as a higher separation of FAA- and FAA+

populations, likely from the enhanced avidity conferred by multivalent antigen presentation (**Figure 4C, Supplementary Figure 8**). One potential limitation of the FAA approach is that covalent ligation reactions may prove difficult with entities of very high molecular weight or structural complexity. Peptide epitopes are often ligated with ease into FAAs due to the peptide's molecular simplicity, but linear peptides cannot present conformational B cell epitopes. The use of full protein antigens on FAAs, as we have shown here, enables the specific labeling of conformation-specific B cell receptors.

FAAs are produced by a two-step conjugation scheme that yields ready-to-use fluorescent constructs that can be aliquoted and stored for use. Compared to other methods such as the subsequent labeling of biotinylated antigen plus streptavidin in series, our front-loaded production blueprint may cumulatively save time during antibody labeling, as FAAs may be used in parallel during labeling with other fluorescent antibodies in a single step. While the use of FAAs was demonstrated in murine cells for this work, the principles should likewise apply in human applications, though application-specific assay development and optimization should be conducted.

ACKNOWLEDGMENTS:

We thank Colette Worcester for help with data collection. This work was supported by the PhRMA Foundation (JDG), the National Science Foundation Graduate Research Fellowship Program (KDA), and by NIH grants R21AI143407, R21AI144408, and DP5OD023118 .

DISCLOSURES:

CJB is co-founder of Orion Bioscience, Inc., a company licensing the SAgA technology for investigating its therapeutic uses. This report is based upon work supported by the National Science Foundation Graduate Research Program under Grant No. 1946099. Any opinions, findings, and conclusions or recommendations expressed in this material are those of the authors and do not necessarily reflect the views of the National Science Foundation.

REFERENCES:

1. Murphy, K., Weaver, C. *Janeway's Immunobiology*. Garland Science. (2016).
2. Sospedra, M., Martin, R. *Immunology of Multiple Sclerosis*, Seminars in Neurology, Thieme Medical Publishers. 115-127. (2016).
3. Knutson, K. L., Disis, M. Tumor antigen-specific T helper cells in cancer immunity and immunotherapy. *Cancer Immunology, Immunotherapy.* **54** (8), 721-728 (2005).
4. Rivino, L. et al. Hepatitis B virus–specific T cells associate with viral control upon nucleos (t) ide-analogue therapy discontinuation. *The Journal of Clinical Investigation.* **128** (2), 668-681 (2018).
5. Constantin, C. M., Bonney, E. E., Altman, J. D., Strickland, O. L. Major histocompatibility complex (MHC) tetramer technology: an evaluation. *Biological Research For Nursing.* **4** (2), 115-127 (2002).
6. Griffin, J. D., Song, J. Y., Sestak, J. O., DeKosky, B. J., Berkland, C. J. Linking autoantigen properties to mechanisms of immunity. *Advanced Drug Delivery Reviews.* (2020).

7. Moody, M. A.; Haynes, B. F. Antigen-specific B cell detection reagents: use and quality control. *Cytometry A.* **73** (11), 1086-1092 (2008).
8. Boonyaratanakornkit, J.; Taylor, J. J. Techniques to study antigen-specific B cell responses. *Frontiers in Immunology.* **10** (1694), (2019).
9. Newman, J., Rice, J. S., Wang, C., Harris, S. L., Diamond, B. Identification of an antigen-specific B cell population. *Journal of Immunological Methods.* **272** (1), 177-187 (2003).
10. Smith, M. J. et al. Silencing of high-affinity insulin-reactive B lymphocytes by anergy and impact of the NOD genetic background in mice. *Diabetologia.* **61** (12), 2621-2632 (2018).
11. Griffin, J. D. et al. Acute B-cell inhibition by soluble antigen arrays is valency-dependent and predicts immunomodulation in splenocytes. *Biomacromolecules.* **20** (5), 2115-2122 (2019).
12. Hartwell, B. L. et al. Antigen-specific binding of multivalent soluble antigen arrays induces receptor clustering and impedes B cell receptor mediated signaling. *Biomacromolecules.* **17** (3), 710-722 (2016).
13. Hartwell, B. L., Pickens, C. J., Leon, M., Berkland, C. Multivalent soluble antigen arrays exhibit high avidity binding and modulation of B cell receptor-mediated signaling to drive efficacy against experimental autoimmune encephalomyelitis. *Biomacromolecules.* **18** (6), 1893-1907 (2017).
14. Hartwell, B. L. et al. Soluble antigen arrays disarm antigen-specific B cells to promote lasting immune tolerance in experimental autoimmune encephalomyelitis. *Journal of Autoimmunity.* **93,** 76-88 (2018).
15. Hartwell, B. L. et al. Molecular dynamics of multivalent soluble antigen arrays support a two-signal co-delivery mechanism in the treatment of experimental autoimmune encephalomyelitis. *Molecular Pharmaceutics.* **13** (2), 330-343 (2016).
16. Kuehl, C. et al. Pulmonary administration of soluble antigen arrays is superior to antigen in treatment of experimental autoimmune encephalomyelitis. *Journal of Pharmaceutical Sciences.* **106** (11), 3293-3302 (2017).
17. Leon, M. A. et al. Soluble antigen arrays displaying mimotopes direct the response of diabetogenic T Cells. *ACS Chemical Biology.* **14** (7), 1436-1448 (2019).
18. Leon, M. A. et al. Soluble antigen arrays for selective desensitization of Insulin-Reactive B cells. *Molecular Pharmaceutics.* **16** (4), 1563-1572 (2019).
19. Sestak, J. O., Fakhari, A., Badawi, A. H., Siahaan, T. J., Berkland, C. Structure, size, and solubility of antigen arrays determines efficacy in experimental autoimmune encephalomyelitis. *The AAPS Journal.* **16** (6), 1185-1193 (2014).
20. Sestak, J. O. et al. Codelivery of antigen and an immune cell adhesion inhibitor is necessary for efficacy of soluble antigen arrays in experimental autoimmune encephalomyelitis. *Molecular Therapy-Methods & Clinical Development.* **1,** 14008 (2014).
21. Thati, S. et al. Routes of administration and dose optimization of soluble antigen arrays in mice with experimental autoimmune encephalomyelitis. *Journal of Pharmaceutical Sciences.* **104** (2), 714-721 (2015).
22. Johnson, S. N. et al. Multimeric insulin desensitizes insulin-specific B cells. *ACS Applied Bio Materials.* (2020).
23. Griffin, J. D. et al. Antigen-specific immune decoys intercept and exhaust autoimmunity to prevent disease. *Biomaterials.* **222,** 119440 (2019).
24. Hartwell, B. L. et al. Multivalent nanomaterials: learning from vaccines and progressing to

antigen-specific immunotherapies. *Journal of Pharmaceutical Sciences.* **104** (2), 346-361 (2015).
25. Laemmli, U. K., Cleavage of structural proteins during the assembly of the head of bacteriophage T4. *Nature.* **227** (5259), 680-685 (1970).
26. Simpson, R. J. Staining proteins in gels with coomassie blue. *CSH Protocols.* **2007,** pdb. prot4719-pdb. prot4719 (2007).
27. Moosmann, A., Müller, E., Böttinger, H. Purification of PEGylated proteins, with the example of PEGylated lysozyme and PEGylated scFv. *Methods Molecular Biology.* **1129,** 527-538 (2014).
28. Haugland, R. P., Coupling of monoclonal antibodies with fluorophores. In *Monoclonal Antibody Protocols*, Davis, W. C., Ed. Humana Press: Totowa, NJ. 205-221 (1995).
29. Martin, T. J., Whalen, M. M. Exposures to the environmental toxicants pentachlorophenol (PCP) and dichlorodiphenyltrichloroethane (DDT) modify secretion of interleukin 1-beta (IL-1β) from human immune cells. *Archives of Toxicology.* **91** (4), 1795-1808 (2017).
30. Felton, J. L., Maseda, D., Bonami, R. H., Hulbert, C., Thomas, J. W. Anti-insulin B cells are poised for antigen presentation in type 1 diabetes. *The Journal of Immunology.* **201** (3), 861-873 (2018).
31. Griffin, J. D. et al. Tocopherol emulsions as functional autoantigen delivery vehicles evoke therapeutic efficacy in experimental autoimmune encephalomyelitis. *Molecular Pharmaceutics.* **16** (2), 607-617 (2019).
32. Yarkoni, Y., Getahun, A., Cambier, J. C. Molecular underpinning of B-cell anergy. *Immunology Reviews.* **237** (1), 249-263 (2010).
33. Pickens, C. J., Johnson, S. N., Pressnall, M. M., Leon, M. A., Berkland, C. J. Practical considerations, challenges, and limitations of bioconjugation via azide–alkyne cycloaddition. *Bioconjugate Chemistry.* **29** (3), 686-701 (2017).
34. Song, J. Y. et al. Glatiramer acetate persists at the injection site and draining lymph nodes via electrostatically-induced aggregation. *Journal of Controlled Release.* **293**, 36-47 (2019).
35. van Dongen, M. A. et al. Avidity mechanism of dendrimer–folic acid conjugates. *Molecular Pharmaceutics.* **11** (5), 1696-1706 (2014).
36. Hudson, P. J., Kortt, A. A. High avidity scFv multimers; diabodies and triabodies. *Journal of Immunological Methods.* **231** (1), 177-189 (1999).
37. Baker, J. C. et al. Selective acylation of epsilon-amino groups. Google Patents: 2003.
38. Grimsley, G. R., Scholtz, J. M., Pace, C. N. A summary of the measured pK values of the ionizable groups in folded proteins. *Protein Science.* **18** (1), 247-251 (2009).
39. Fesel, C., Coutinho, A. Serum IgM repertoire reactions to MBP/CFA immunization reflect the individual status of EAE susceptibility. *Journal of Autoimmunity.* 14 (4), 319-324 (2000).

All figures and supplementary figures are now uploaded under the preferred .svg extension

Figure 1

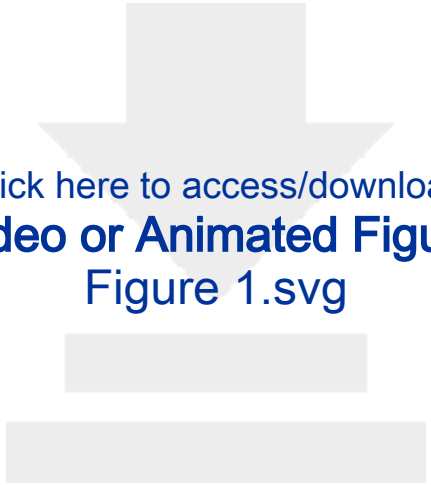

Click here to access/download

Video or Animated Figure

Figure 1.svg

Figure 2

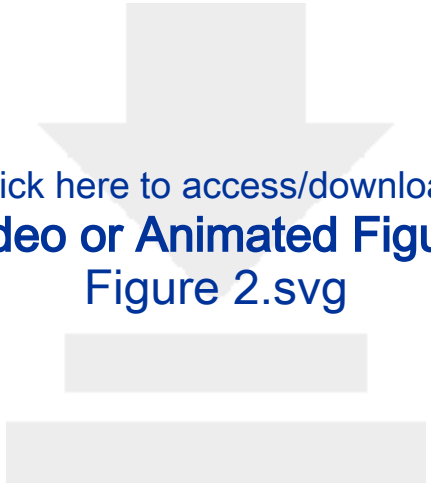

Click here to access/download

Video or Animated Figure

Figure 2.svg

Figure 3

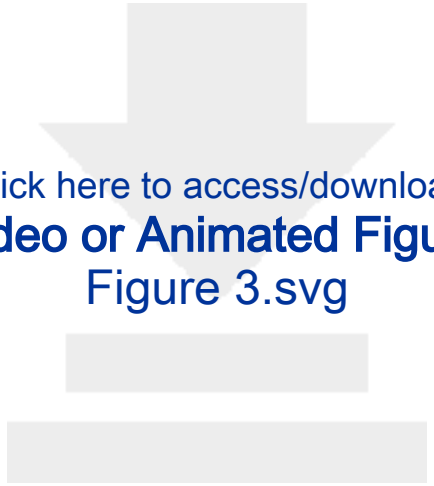

Click here to access/download

Video or Animated Figure

Figure 3.svg

Figure 4

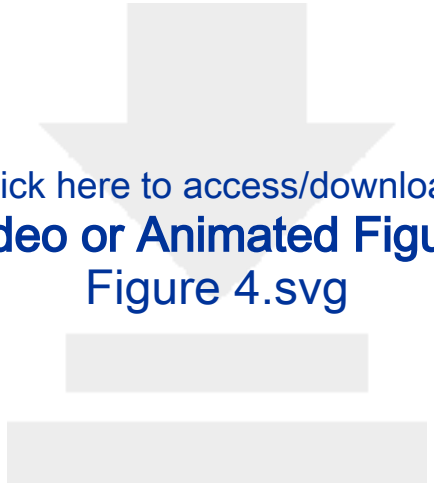

Click here to access/download

Video or Animated Figure

Figure 4.svg

Figure 5

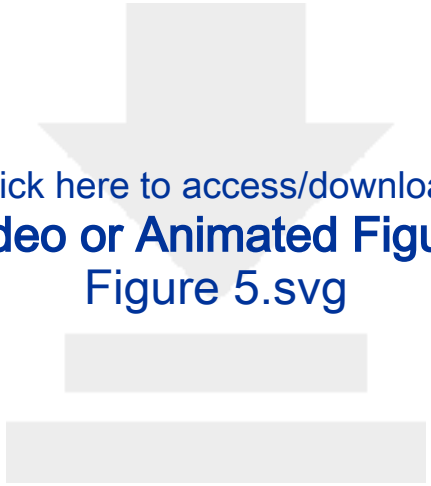

Click here to access/download

Video or Animated Figure

Figure 5.svg

Supplementary Figure 1

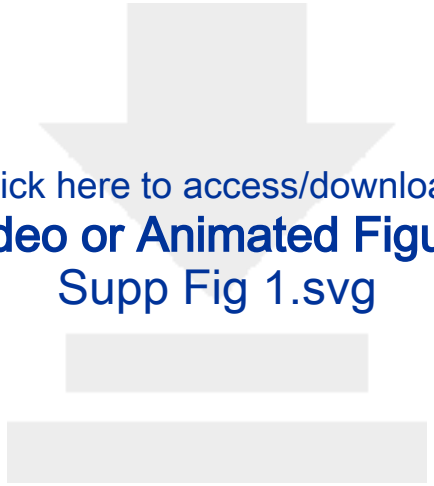

Click here to access/download

Video or Animated Figure

Supp Fig 1.svg

Supplementary Figure 2

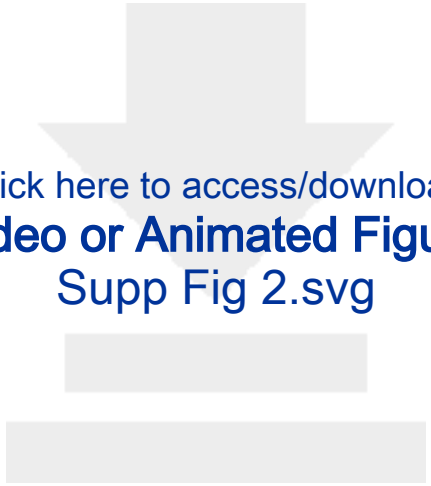

Click here to access/download

Video or Animated Figure

Supp Fig 2.svg

Supplementary Figure 3

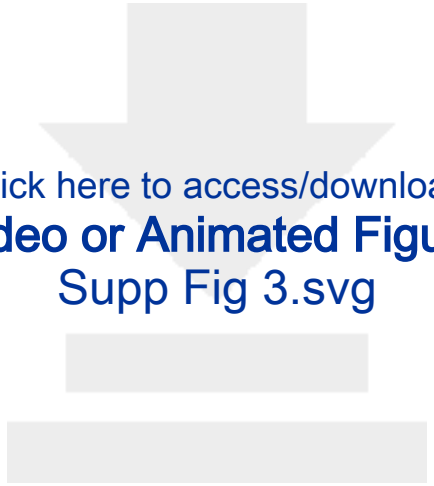

Click here to access/download

Video or Animated Figure

Supp Fig 3.svg

Supplementary Figure 4

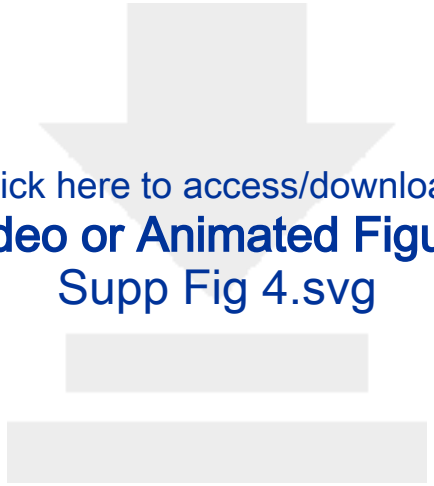

Click here to access/download

Video or Animated Figure

Supp Fig 4.svg

Supplementary Figure 5

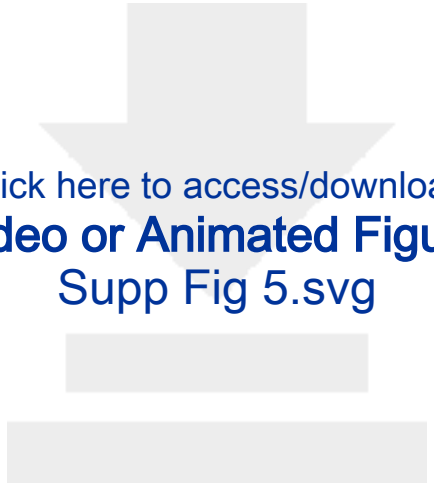

Click here to access/download

Video or Animated Figure

Supp Fig 5.svg

Supplementary Figure 6

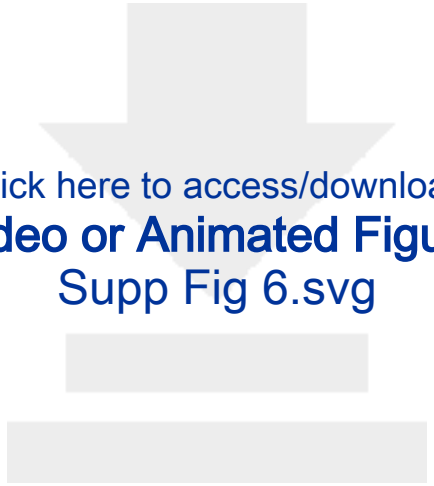

Click here to access/download

Video or Animated Figure

Supp Fig 6.svg

Supplementary Figure 7

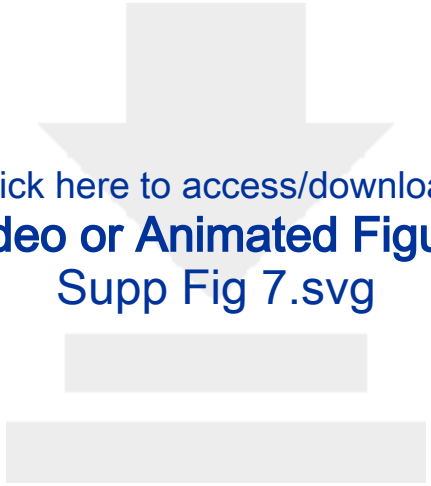

Click here to access/download

Video or Animated Figure

Supp Fig 7.svg

Supplementary Figure 8

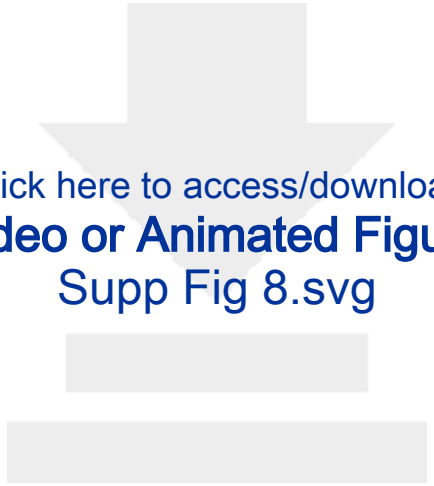

Supplementary Figure 9

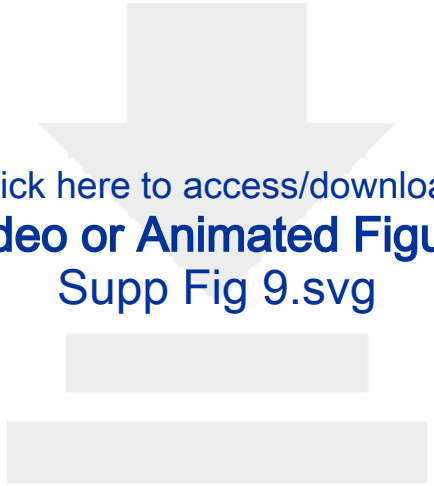

Click here to access/download

Video or Animated Figure

Supp Fig 9.svg

Supplementary Figure 10

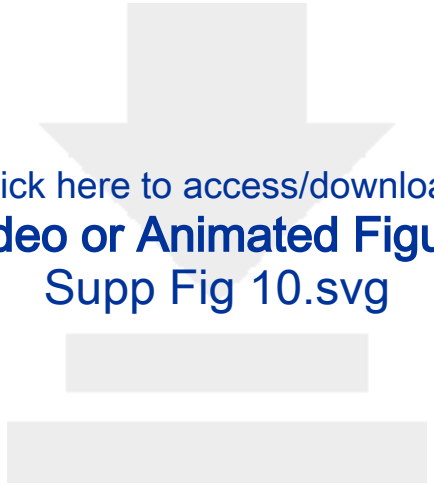

Click here to access/download

Video or Animated Figure

Supp Fig 10.svg

Supplementary Figure 11

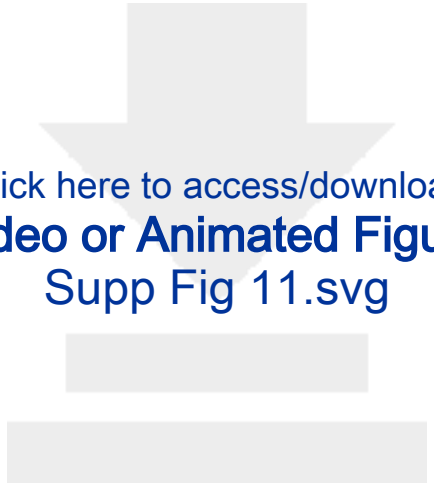

Click here to access/download

Video or Animated Figure

Supp Fig 11.svg

Name of Material/ Equipment	Company	Catalog Number
1,1,3,3-tetramethylguanidine	Alfa Aesar	AAA12314AC
12 M hydrochloric acid	Fisher Chemical	A508-4
12% Mini-PROTEAN TGX Precast Protein Gels, 10-well, 30 ul	Bio-Rad	4561043
20 kDa 4-arm PEG azide	Jenkem USA	A7185-1
3.5 kDa MWCO dialysis tubing (regenerated cellulose)	Fisher Scientific	25-152-10
Acetonitrile, HPLC grade	Fisher Chemical	A998-4
Alexa Fluor 647 anti-mouse CD19 Antibody	BioLegend	115522
anhydrous dimethylsulfoxide	ACROS Organics	AC610420010
barium chloride	ACROS Organics	203135000
Brilliant Blue G-250 Dye	Fisher BioReagents	BP100-50
Cell Prime r-insulin	EMD Millipore	4512-01
Copper (II) sulfate pentahydrate	ACROS Organics	AC197722500
dimethylsulfoxide	Fisher Chemical	S67496
fluorescein isothiocyanate (FITC) isomer 1	Sigma-Aldrich	F7250-1G
Glacial acetic acid	Fisher Chemical	A38-212
Glycerol	ACROS Organics	15892-0010
Glycine	Fisher Chemical	G46-500
homopropargyl-PLP	Biomatik	NA
iodine	Sigma-Aldrich	207772-100G
Methanol, HPLC grade	Fisher Chemical	A452-4
NHS-Rhodamine (5/6-carboxy-tetramethyl-rhodamine succimidyl ester), mixed isomer	Thermo Scientific	46406
PE/Cyanine7 anti-mouse CD3 Antibody	BioLegend	100220
potassium iodide	Sigma-Aldrich	30315
propargyl N-hydroxysuccinimide ester	Sigma-Aldrich	764221
sodium ascorbate	Sigma-Aldrich	A7631
sodium biocarbonate	Sigma-Aldrich	S5761-1KG
sodium dodecyl sulfate	Fisher BioReagents	BP166-100
Sodium phosphate monobasic monohydrate	Fisher Chemical	S468-500
trifluoroacetic acid	Sigma-Aldrich	302031-10x1mL
Tris base	Fisher BioReagents	BP152-500

Tris(3-hydroxypropyltriazolylmethyl)amine	ClickChemTools	1010-1000
xBridge BEH C18 3.5 um, 4.6 x 150 mm column	Waters	186003034
xBridge BEH C18 5um OBD Prep Column, 19 x 250 mm	Waters	186004021

Comments/Description
Recombinant human insulin for insulin FAA synthesis
Custom synthesis (sequence: homopropargyl-HSLGKWLGHPDKF; purity: 97.29%)
A commercially available analog of the Rhodamine-B NHS ester used in the paper

Editorial comments:
Changes to be made by the Author(s):

1. Please take this opportunity to thoroughly proofread the manuscript to ensure that there are no spelling or grammar issues.
We reviewed the manuscript and corrected the issues.

2. Please remove the embedded Table from the manuscript.
We removed the table and will include it separately.

3. Please highlight up to 3 pages of the Protocol (including headings and spacing) that identifies the essential steps of the protocol for the video, i.e., the steps that should be visualized to tell the most cohesive story of the Protocol. Remember that non-highlighted Protocol steps will remain in the manuscript, and therefore will still be available to the reader.
We highlighted key steps for the video, particularly for the synthesis of fluorescent antigen arrays.

4. Please ensure that the highlighted steps form a cohesive narrative with a logical flow from one highlighted step to the next. Please highlight complete sentences (not parts of sentences). Please ensure that the highlighted part of the step includes at least one action that is written in imperative tense.
Confirmed.

Reviewers' comments:
Reviewer #1:

Manuscript Summary:
This manuscript titled 'Tetrameric fluorescent antigen arrays for single-step identification of antigen-specific B cells' presents a previously used method for the application of 'baiting' antigen-specific B cells. The isolation of antigen-specific B cells is difficult due to the scarcity of specific cells and the unavailability of efficient reagents. In that regard, this protocol provides an additional method to scientists in the B cell field.

Major Concerns:

A deeper discussion on the benefits and shortcomings of this method would be valuable. The examples shown are for murine cells; whether this method can as easily be applied to human studies has not been clearly established.
We agree and we added a new final paragraph to the discussion addressing these points in comparison to another conventional B cell labeling modality. We now confirm that these principles should also be applicable for the study of human samples (Lines 431-439).

Minor Concerns:
1. Troubleshooting pointers after steps 1 and 2 would help.
This is an excellent suggestion to improve accessibility to the protocol. We added several new troubleshooting sentences to the discussion in Step 1.1, 1.3, and 2. (Lines 380-386, 394-397)

2. Please provide stability and storage guidance for product after step 2.

We updated the manuscript to include our specifications for appropriate storage and stability (Lines 121-124, 144-151, 165-168).

3. The figures 1 and 2 have not been cited anywhere in the paper.

The omission has been corrected and figures 1 and 2 are now cited in the manuscript (Lines 78, 292-297, 371).

4. The Figure legend for Fig2 has a typo.

We corrected the spelling of fluorophore (Line 453).

5. The statistical tests used to establish significant differences are not mentioned.

We thank the reviewer on this point and we now include information about statistical tests in the figure legends for Figs. 4 & 5, and also Supp. Fig. 10. (Lines 473-474, 480-482, 539)

6. For some figures the 'n' or the number of times the experiment was done is not provided.

We now ensure that replicate numbers are appropriately included with figure and supplementary figure captions. (Lines 473, 481, 539)

Reviewer #2:

Manuscript Summary:

The authors present a protocol for staining and analyzing antigen-specific B cells utilizing a flow cytometry-based platform. Such analyses are critical for understanding immune activation in a variety of systems. We believe the article may be suitable for publication in JoVE, pending some revisions and technical specifications for the protocol.

Major Concerns:

NONE

Minor Concerns:

*** Gentle heating at what temperature? Reduced pressure at what pressure? Please list details of the temperature during heating, and settings on the rotavap.**

We thank the reviewer for these points, and we added specific temperature instructions to Step 1.1., and pressure and rotation specifications to Step 1.2.1. (Lines 106, 121)

*** Would be great to include notes on the physical characteristics of the resulting functionalized antigens: stability, hygroscopic, storage conditions if applicable (does it need to be kept under inert gas, etc)**

We now include the suggested storage conditions to the functionalized antigen in Step 1.2.1, and for the antigen array in Step 1.4.1. We added additional notes on hygroscopicity and stability as well (Lines 121-124, 138-151, 165-168)

*** At what temperature is the dialysis done? Room temperature or 4C?**

We now specify dialysis temperature (Line 162)

*** Suggest including short protocol for isolation of B cells from blood or other commonly used tissue as**

a prep example (are there any considerations to be made prior to preparation? Is this compatible with enzymatic digestion of tissues?)

We included a note citing supplementary protocols for blood and spleen isolation. We try to avoid enzymatic digestion because it has the potential to alter cell surface proteins including the BCR and key clusters of differentiation that are used for flow cytometry. We also include a note (Lines 223-225).

*** Antibody titers?**

All fluorescent antibody assays were conducted under manufacturer recommended working concentrations, which we confirmed were appropriate for our experiments (Lines 247-248). We have added an additional note to remind all researchers to titrate each antibody batch received to confirm its efficacy (250-251).

*** The FAA titers seem quite high as most kits start 1 - 5 micrograms, would suggest providing a titer that covers the low end (ex. starting at 0.5)**

In this demonstration we provide a sample set of FAA titers. We agree that FAA concentrations can vary depending on user-specified applications.

*** Fig 4D/ Supp Fig 8: Why was the comparison not made with commercially available monovalent insulin-fluorescent product? That may have provided a more accurate benefit analysis in the context of used concentrations/test.**

We compared FAAs to an insulin-fluorophore conjugate because we could fully characterize it and confirm its exact identity, and also to keep the attachment point on insulin (B29 lysine) as the exact same between monovalent and multivalent materials. This specification eliminated the variable for any improvement or reduction in activity being due to a different site of modification that may allow better access to, or hinder the accessibility, of the epitope region on insulin. We know modification at the B29 lysine does not block any major B cell epitopes of insulin, and thus we believe the monomeric insulin-fluorophore that we made in-house is superior to commercially available fluorescent insulin alternatives, and is also the most accurate monomeric control available for our experiments.

*** Fig 4: Specify the source of cells**

We added this information to the representative results section (Lines 330-334).

*** Specify the statistic used alongside p-values (ex. Students T-test, ANOVA)**

We corrected the omission and added this information to figure captions. (Lines 473-474, 480-482, 539)

*** Supp Fig 4: make SSC-A linear, a log-scale is not needed on a splenocyte plot especially when gating lymphocytes.**

We thank the reviewer for this guidance and adjusted Supp. Fig. 4 accordingly.

*** Supp Fig 4: The FSC-H x FSC-W plot should be linear, and the FSC-H x FSC-A plot should follow along a y = x line, if not, area scaling should be adjusted in the cytometer to ensure a y = x singlet angle. The FSC-H x FSC-W plot should be a flat line (no angle)**

We adjusted the singlet plot representation accordingly.

*** Please remove log scale from both panels A and B, there is unnecessary compression of events into a very small portion to the graph. FSC and SSC (-A, -H, -W) should be in linear scale. Only very messy**

samples with very different cell populations (ex.tumors looking at both lymphocytes and fibroblasts) benefit from log, for all others data and information is lost.

These plots are now in linear scale, and we thank the reviewer for this guidance.

*** ALL FIGURES: Text compression in figures with FACS plots (might have been through submission site) has make the text illegible and pixelated**

We appreciate the notification that this loss of resolution has occurred. We will work with the editor to ensure that the figures are translated with full integrity for the final publication.

*** ALL FACS Plots: Include fluorescence minus one controls**

We performed extensive single-stain controls on our small flow panel marker, which was designed for minimal spectral overlap, with the only critical overlap (CD3-PE/Cy7 → CD86-PE) designed to be on those markers because CD3 is marker for non-B cells in this flow panel (i.e., a dump gate), and that known spectral overlap does not influence our data or conclusions. Upon further close analysis at the suggestion of the reviewer, we did observe minor spectral overlap from the CD86-PE channel into PerCP-5.5 (CD79b) – but importantly, not in the reverse direction – and we have removed CD79b results from the report accordingly. As the reviewer notes, FACS controls are critical for our analysis and we now include a new supplementary figure showing single-stain controls that substantiate our gating strategy (Supp. Fig. 10).

We also note that critical markers in adjacent channels such as FAA-FITC and CD86-PE exhibited opposite staining trends, which was consistent with appropriate biological activity and demonstrated that these channels measured cell surface markers independently of each other. For example, FITC+ events decreased between vehicle and antigen treatment groups, while CD86 signals increased between vehicle and antigen treatment groups (Fig. 5 and Supp. Fig. 11). We included a new note in the assay development section (Step 4) for researchers to include additional controls to validate of their chosen assay, especially if using an expanded number of flow markers (Lines 239-240). We thank the reviewer for emphasizing the importance of flow marker panel design and validation.

*** Supp Table 1: Clean up formatting to match the other figures**

Thank you for the catch. We resolved the discrepancy.

Reviewer #3:

Manuscript Summary:

The manuscript by Apley et al., entitled "Tetrameric fluorescent antigen arrays for single-step identification of antigen-specific B cells" described a general method to prepare tetrameric fluorescent antigen arrays for characterizing antigen-specific B cells by flow cytometry. The authors explored an azide-alkyne click chemistry that enables conjugating a couple of model antigens to four arm PEG-Azide backbone molecules to produce tetrameric antigen array, followed by conjugation of fluorophore to the antigen array which resulted in fluorescent antigen arrays for B cell response analysis. The authors subsequently used the fluorescent antigen arrays to characterize B cell responses in two mouse models, the VH125 NOD mouse model for type 1 diabetes, and the EAE mouse model for multiple sclerosis. The authors showed that the tetrameric fluorescent antigen arrays are superior to monomeric fluorescent antigen in identifying antigen-specific B cells by increasing the sensitivity which resulted in a larger detectable antigen-specific B cell population. Furthermore, the identification of antigen-specific B cell population allows assessment of antigen-specific B cell activation induced by ex vivo antigen stimulation. Overall, the study described in the manuscript is well thought out. The experiments are well controlled and the data are solid. The

method described here, which is an advancement for studying B cell response in various settings including vaccination and autoimmunity, will be valuable for the field. Some suggestions are listed as below to improve the clarity and precision for publication.

Major Concerns:

The rationale of each FAA could be explained specifically in the introduction section so that the reader can easily understand the scope of this manuscript. For instance, why insulin and PLP are selected as model antigens in this manuscript. Lines 295-301 did some job. However, it is better to put this part in the introduction section.

We thank the reviewer for this suggestion. We modified our introduction to clearly state our intention and the models used (Lines 88-94).

Minor Concerns:

1) Figure 1 and 2 have not been mentioned in the main text.

We corrected the omission and Figures 1 and 2 are now cited in the manuscript (Lines 78, 292-297, 371).

2) What is FITC-PLP (line 279)? PLP was first mentioned on line 279 without spelling out the full name. The full name of PLP is explained on line 296, instead. Please reverse the order. The same with EAE, without fully spelling out in any section of the manuscript.

We thank the reviewer and now introduce the antigens and models within the introduction for clarity (Lines 88-94).

3) Fig. 4 and 5, Fig. S10, what statistical method is used to report the p value?

We now include statistical analysis details (unpaired, two tailed t tests) for all comparisons within the captions for each figure (Lines 473-474, 480-482, 539).

4) Fig. S7 c and d, the Y-axis are labeled as "PE% of CD19+ cells). However, it is described in the figure legend that Rhodamine 4-arm PLP is used to labeled cells. The description of the fluorophore should be consistent.

We thank the reviewer for noticing this. The rhodamine dye is detected in the PE channel, but it is appropriate to rename the populations “%RhdB+”, consistent with our dye, and we updated Fig. S7 for clarity.

5) Fig. S8, left panel, what does the blue gate mean? Please specify.

. We updated the figure caption to state the purpose of the blue gate denoting insulin-specific B cells that are identified by FAAs but not by monovalent insulin (Lines 518-520).

6) Fig. S10 shows PLP-specific B cells. PLP is labeled with Rhodamine in the text, however, the figure lists FITC+ of CD19+ population. The label is not consistent with the text.

In Fig. S10 (now Fig. S11) we used the FITC 4-arm PLP variant because FITC was more compatible with the labeling antibodies used. We updated the representative results and discussion sections accordingly (Lines 351, 428-429).

Reviewer #4:

Manuscript Summary:

This manuscript is about the use of fluorescent-conjugated antigens to track down antigen-specific B

cells. More specifically, the authors present a 2-step protocol that would significantly enhance the detection of these cells through the usage of a 4-arm-fluorochrome-labelled antigen in comparison to a monovalent counterpart.

Major Concerns:
None.

Minor Concerns:
Described below point-by-point.
It would be interesting to include the entire time spent in that each step of the whole protocol.

Time estimates are an excellent idea and we appreciate the suggestion. We now include these estimates throughout the steps presented, and also for many sub-steps.

Line 99 - It is not clear what the authors meant by functionalizing a native antigen. Please, give details about it.

We substituted "native" for "unmodified" (Line 104).

Line 118 - It is not clear how the antigen array can be synthesized by copper-catalyzed, azide-alkyne cycloaddition (CuAAC). Please, give details about it.

We cite a prior report on CuAAC conjugation to provide additional details (Line 126-127, Ref 22)

All figures must be presented in a higher-resolution format. Some of them were simply impossible to evaluate, specially to read any of the details added, such as shown in the Figure 4D and Supplementary Figures 5 and 6.

We appreciate the notification that this loss of resolution has occurred. We will work with the editor to ensure that the figures are translated with full integrity for the final publication.

Supplem Fig 3 - I suggest to change the line color for the insulin antigen array to clearly distinguish it from the FITC PLP FAA curve. Also, I suggest to include the curve of PLP antigen array in this figure as an important control.

Thank you for the recommendation to help improve the clarity of the figure. The PLP antigen array curve has been included and the color pallet has been changed to allow individual species to be better distinguished.

Figures 4A, 4B and 4C - Although it is clear the improvement on the B cell staining with a lower FITC 4-arm insulin and no effect over T cells, no isotype Ab control was added to the staining. This data should be shown as is plus the addition of control staining side by side, which would highlight the quality of the cell staining.

Isotype controls were not required for this particular demonstration because FAA+ populations were compared relatively between two cell populations (CD19 as specific, CD3 as nonspecific), and both these antibodies have the same mouse kappa isotype. We primarily intended our cytometry data as a baseline demonstration for researchers to adapt for their own purposes. We have included a new note in the assay development section of the protocol for researchers to include additional controls for full validation of their chosen assay. (Lines 239-240)

Supplementary Figures 7A and 7C - I suggest to use the same y-axis scale for both panels (left and right) of each figure.

We adjusted the y-axis scaling to be consistent between each panel.

Supplementary Figures 9A-B - I disagree that FAA- and FAA+ B cell subsets were completely separated with the chosen gating strategy. Indeed, the displayed plots do not show FAA+ (4-arm FITC) cells totally separated from the FAA- counterparts. As suggested for Figure 4 data, I suggest to include data from control stainings, such as isotype Ab control.

We agree that these subsets were not completely separated from one another in the plots we obtained after 24 hours, unlike in the specificity studies with fresh cells (Supp. Fig. 8). As such, we have tempered our assertion in the representative results when reporting the data from the functional assays (Lines 351-355). We also included a new supplementary figure (S10) providing control staining used for gating.

Figure 5 and Supplementary Figure 10 - there is no explanation in the manuscript about why it is relevant to verify the expression of CD86+ and CD79b+ in the antigen-specific B cells, neither the details of treatment performed to stimulate the up- or down-regulation of these costimulatory molecules. About the gating strategy for CD86+ and CD79b+, it must be presented as done in the Figure 4. Also, there are no information about the anti-CD86 and anti-CD79b antibodies used in this cell staining procedure. Furthermore, authors focused on the respective MFIs for both CD86+ and CD79b+ FAA+ stainings. What about the absolute number of CD86+ and CD79b+ FAA+ elicited between the vehicle and the insulin or PLP treatment? Does this parameter also change as seen with the MFIs?

While we intended the assays in these figures as supplementary demonstrations of the potential utility for FAAs, we certainly hope to avoid adding additional confusion by introducing additional markers. We have briefly described our study and rationale for looking at these phenotypical markers as examples for observing changes to antigen-specific B cells in response to stimulation and treatment conditions (Lines 351-355, 357-362). References 22 and 31 are also included to substantiate marker selection.

We have included the source information for fluorescent antibodies in the representative results section (Line 359), but not the materials table as this experiment is complementary but not essential to the instruction of this methods paper. We did not gate for CD86 (or CD79b) positive populations – B cells all express varying levels of these markers on a continuous scale, and therefore we focused on MFI for this analysis.

Once formed a 4-arm antigen fluorochrome, any idea about how much time the conjugated fluorescence can be maintained on this antigen? When compared to other methods, this 2-step procedure induces a more stable antigen for cell staining?

Proper storage of the FAAs in -20 °C and dry atmosphere will keep FAAs stable for several months. As long as they are stored in the dark, the fluorophore will not photobleach. Using irreversible conjugation chemistries, like the NHS-ester, forms an amide bond that is not readily hydrolyzed. We have included information on product stability in the updated protocol (Lines 122-124, 144-151, 165-168).

We have not performed a direct comparison in this study, but Ref 8 notes that conventional streptavidin tetramerization methods sometimes induce deleterious aggregation that may be avoided using soluble, polymeric backbones that are stored as a fully conjugated construct.

Supplementary Table 1

Click here to access/download;Supplemental File (Figures, Permissions, etc.);JoVE_Supplementary Table 1.xlsx

Sample ID	E, antigen (280nm)	E, dye (max)	CF	[mg/ml]	280 nm Absorbance	490 nm Absorbance
Insulin AA (0.1 mg/ml)	5734			0.1	0.052	0
PLP AA (0.1 mg/ml)	5500			0.1	0.035	-0.008
FITC Insulin FAA (0.1 mg/ml)	5734	68000	0.3	0.1	0.104	0.186
RhdB Insulin FAA (0.1 mg/ml)	5734	65000	0.3	0.1	0.14	
FITC PLP FAA (0.1 mg/ml)	5500	68000	0.3	0.1	0.165	0.386
RhdB PLP FAA (0.1 mg/ml)	5500	65000	0.3	0.1	0.333	

555 nm Absorbance	Dye/FAA
-0.002	
-0.009	
	1.3
0.099	0.25
	2.54
0.089	0.1